SCIENTIFIC REPORTS

OPEN

SUBJECT AREAS:

BATTERIES

ORGANIC MOLECULES IN MATERIALS SCIENCE

Received
26 September 2014

Accepted
19 November 2014

Published
10 December 2014

Correspondence and requests for materials should be addressed to K.T.L. (ktlee@unist.ac.kr) or C.Y. (yang@unist.ac.kr)

Synthesis of Ordered Mesoporous Phenanthrenequinone-Carbon via π-π Interaction-Dependent Vapor Pressure for Rechargeable Batteries

Mi-Sook Kwon[1], Aram Choi[1], Yuwon Park[1], Jae Yeong Cheon[2], Hyojin Kang[1], Yong Nam Jo[3], Young-Jun Kim[3], Sung You Hong[1], Sang Hoon Joo[1], Changduk Yang[1] & Kyu Tae Lee[1]

[1]School of Energy and Chemical Engineering, Ulsan National Institute of Science and Technology, Ulju-gun, Ulsan, 689-798, South Korea, [2]Department of Chemistry, Ulsan National Institute of Science and Technology, Ulju-gun, Ulsan, 689-798, South Korea, [3]Advanced Batteries Research Center, Korea Electronics Technology Institute, Bundang-gu, Seongnam-si, Gyeonggi-do, 463-816, South Korea.

The π-π interaction-dependent vapour pressure of phenanthrenequinone can be used to synthesize a phenanthrenequinone-confined ordered mesoporous carbon. Intimate contact between the insulating phenanthrenequinone and the conductive carbon framework improves the electrical conductivity. This enables a more complete redox reaction take place. The confinement of the phenanthrenequinone in the mesoporous carbon mitigates the diffusion of the dissolved phenanthrenequinone out of the mesoporous carbon, and improves cycling performance.

In the past few decades, the major energy source globally has been fossil fuels which are non-renewable, finite, and environmentally hazardous. Recently, considerable effort has been devoted to this problem, and clean and sustainable energy systems have been studied including solar cells, fuel cells, and rechargeable batteries. Among them, Li ion batteries are currently the dominant energy storage system in portable electronic devices, hybrid electric vehicles and energy storage systems (ESS)[1,2]. However, the commonly used positive electrode materials in Li-ion batteries are Co-based inorganic compounds such as $LiCoO_2$ and $LiNi_{1-x-y}Co_xMn_yO_2$ prepared from limited mineral resources[3]. Co is costly and toxic. Moreover, the synthesis of these ceramic materials requires high energy consumption such as heating above 700°C. Therefore, there is great demand for new environmentally friendly electrode materials derived from renewable resources with minimum energy consumption. One possible approach is to use organic electrode materials[4–8]. Organic compounds extracted or synthesized from renewable natural products or biomass can provide a sustainable base for realizing Li-ion batteries[9]. For example, lithium terephthalate was suggested as a promising electrode material, because it can be produced either by the oxidative metabolism of p-xylene or by recycling commonly used polyethylene terephthalate (PET) plastic.

Since the first organic electrode based on a small molecule, lithium-dichloroisocyanuric acid, was introduced in 1969[10], various small organic molecules (e. g., oxocarbons, carbonyl compounds, polyketones with N-cycles) have been reported as electrode materials for Li-ion batteries[11–19]. Small molecules are promising candidates because their structural richness enables easy modification of their physical and electrochemical properties. However, small organic compounds suffer from several drawbacks such as their dissolution in organic electrolytes and poor electrical conductivity, resulting in poor cycle performance and reversible capacity.

Recently, several promising strategies have been demonstrated to mitigate the dissolution of organic compounds, including polymerization[20–25], grafting[26–28], salt formation[29,30], and composites with carbon[31–34], giving rise to improved electrochemical performance.

A similar dissolution problem of redox-active materials has been observed in Li-sulfur batteries, and sulfur-confined ordered mesoporous carbon (CMK-3) was recently suggested to trap dissolved polysulfides in the mesopores of carbon, resulting in improved electrochemical performance[35]. Inspired by the use of CMK-3 to inhibit the dissolution of redox-active materials in Li-S batteries, herein, we introduce the simple synthesis of an ordered mesoporous phenanthrenequinone–carbon composite using the new concept of the vapour pressure of

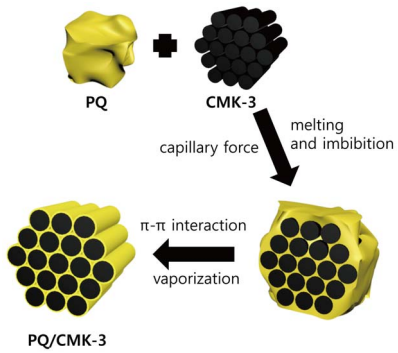

Figure 1 | **Schematic diagram for the synthesis of a phenanthrenequinone (PQ)-confined ordered mesoporous carbon (CMK-3).**

phenanthrenequinone, which is dependent on the π-π interaction between aromatic phenanthrenequinone and carbon. This is the first report of the synthesis of small-organic-molecules-confined ordered mesoporous carbon through the π-π interaction between aromatic phenanthrenequinone and carbon. The confinement of phenanthrenequinone (PQ) in the ordered mesoporous carbon (CMK-3) mitigated the dissolution of PQ in aprotic electrolytes and increased the electrical conductivity because of the intimate contact between carbon and PQ, and therefore, the composite showed the highly improved electrochemical performance including high reversible capacity of approximately 240 mA h g^{-1}, good rate capability delivering 113 mA h g^{-1} at a rate of 2 C, and stable cycle performance with little capacity fading over 50 cycles.

Results

PQ-confined CMK-3 (PQ/CMK-3) was prepared by following a melt-diffusion-vaporization strategy. First, CMK-3 was obtained

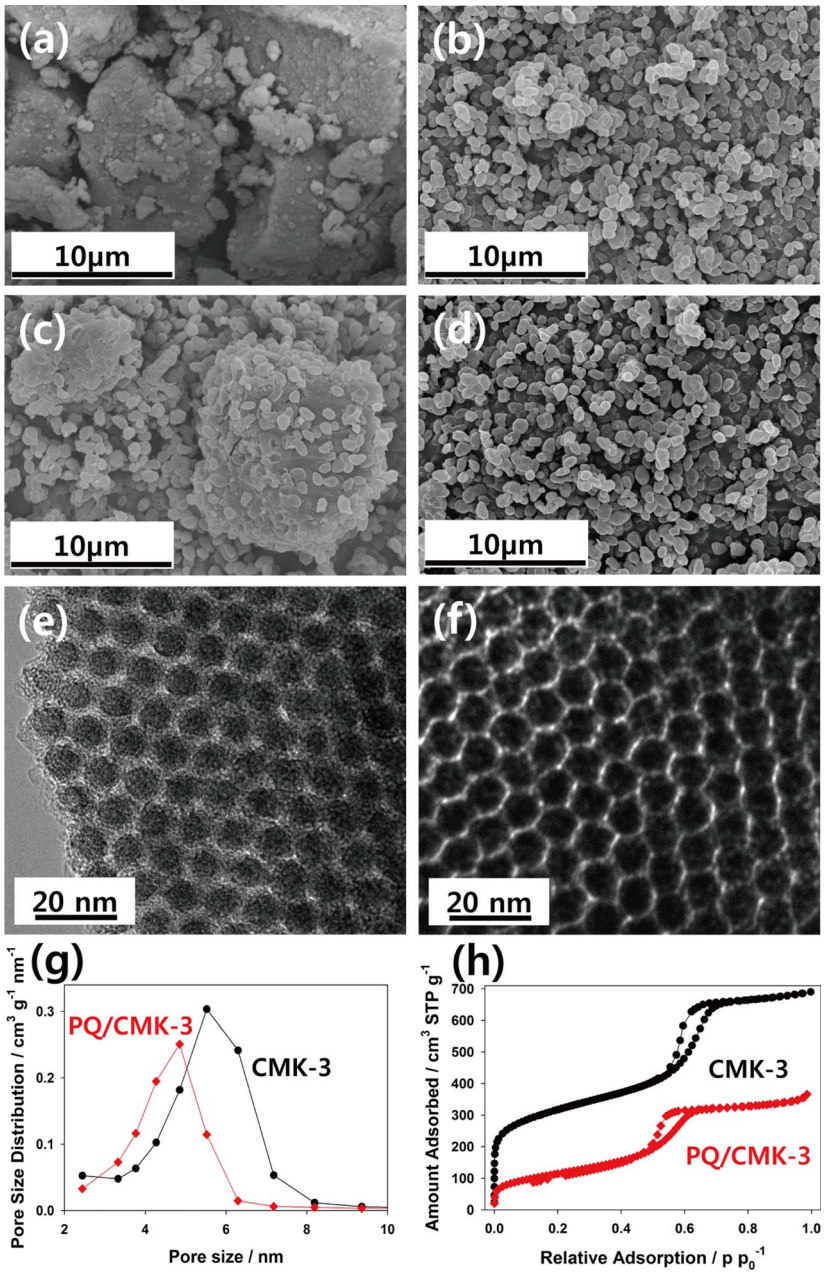

Figure 2 | SEM images of (a) bare PQ, (b) CMK-3, (c) mixture of PQ and CMK-3, and (d) phenanthrenequinone-confined CMK-3 (PQ/CMK-3). HR-TEM images of (e) CMK-3 and (f) PQ/CMK-3. (g) BJH Adsorption pore size distributions and (h) the corresponding nitrogen adsorption-desorption isotherms of CMK-3 and PQ/CMK-3.

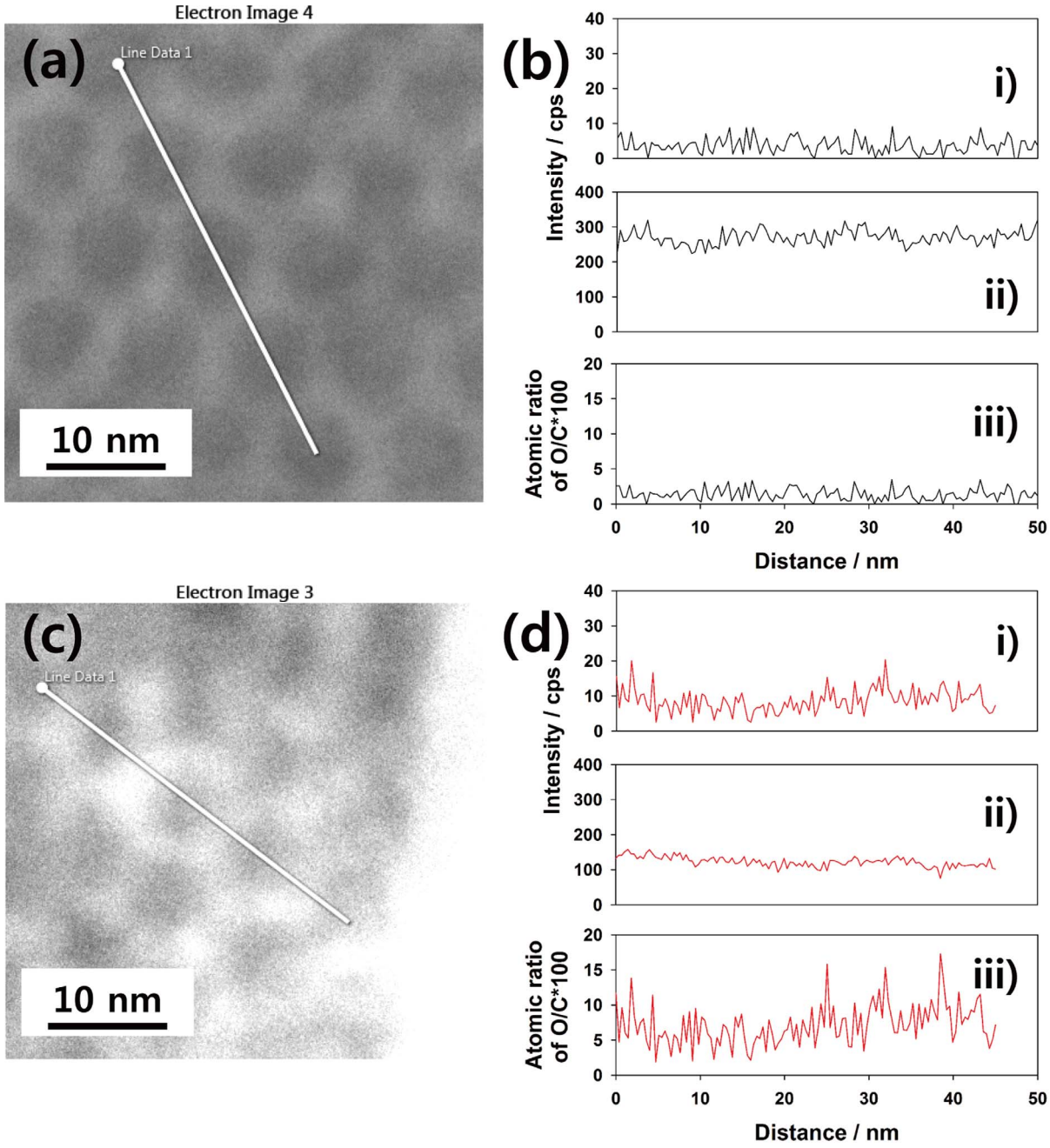

Figure 3 | **TEM images and EDS line profiles of (a, b) CMK-3 and (c, d) PQ/CMK-3: i) oxygen, ii) carbon, iii) oxygen/carbon.**

by a nanocasting method using ordered mesoporous silica (SBA-15) as a hard template. The resulting replica was the two-dimensional hexagonally ordered carbon rods, comprising an assembly of about 7-nm-thick carbon rods separated by empty channel voids about 6 nm wide. Then, a 3 : 1 weight ratio mixture of PQ and CMK-3 was heated at 250°C in air for 3 h between the melting point (ca. 200°C) and boiling point (ca. 360°C) of PQ. The melted PQ was imbibed into the channels by capillary forces. However, only the PQ adsorbed on the surface of the carbon rods in the CMK-3 remained after heating owing to the π-π interaction between the aromatic PQ and CMK-3, whereas the PQ residue without the π-π interaction evaporated and was eliminated with the air flow because of the high vapour pressure of the PQ. Therefore, after cooling, the solidification of PQ formed PQ-confined CMK-3 comprised of carbon-PQ core-shell nanofibers with the intimate contact between them, as shown in Fig. 1. The scanning electron microscopy (SEM) images in Fig. 2 reveal the changes in the mixture of CMK-3 and PQ before and after heating at 250°C. Figs. 2a and b represent bulk PQ and CMK-3, respectively. The bulk PQ was evident in the SEM image of the initial mixture obtained by hand-grinding (Fig. 2c). However, the bulk PQ completely disappeared with no significant fraction on the external surface of CMK-3 after heating at 250°C (Fig. 2d). CMK-3 and PQ are both hydrophobic materials, which account for the incorporation of PQ into the pore channels by capillary forces. The filling of the carbon channels with PQ was supported by the transmission electron microscopy (TEM) images corresponding to the (110) plane, in which the filling of the pores with the PQ is evidenced by the decrease in the pore size of the CMK-3 after filling (Figs. 2e and f). This is further corroborated by the decrease in the Barrett-Joyner-Halenda (BJH) adsorption pore size distribution of the CMK-3 after the incorporation of the PQ (Figs. 2g and 2h). This is consistent with the decrease in the surface area and pore volume after

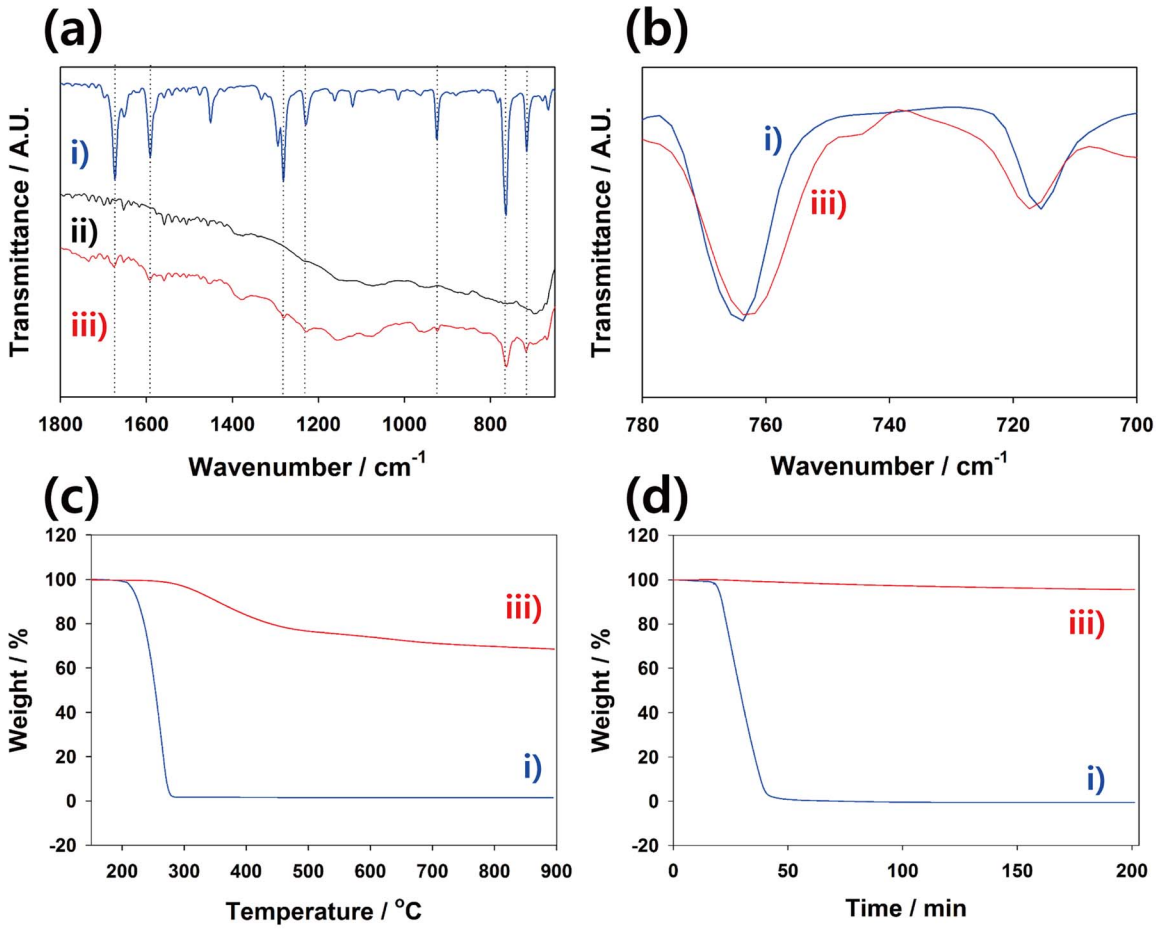

Figure 4 | (a) FT-IR spectra, (b) their enlarged spectra, (c) TGA profiles, and (d) isothermal analysis of i) bare PQ, ii) CMK-3, and iii) PQ/CMK-3.

filling (1118 $m^2 g^{-1}$ and 1.07 $cm^3 g^{-1}$ for CMK-3, and 418.2 $m^2 g^{-1}$ and 0.563 $cm^3 g^{-1}$ for PQ/CMK-3). The presence of residual pores in the PQ/CMK-3 allows ingress of electrolyte, resulting in the facile Li^+ migration within the structure. The oxygen and carbon elemental EDS line profiles also demonstrate that the PQ was homogeneously distributed in the framework of the mesoporous carbon (Fig. 3). The relative oxygen/carbon ratio of PQ/CMK-3 was higher than that of CMK-3, because the PQ, having a higher oxygen/carbon atomic ratio

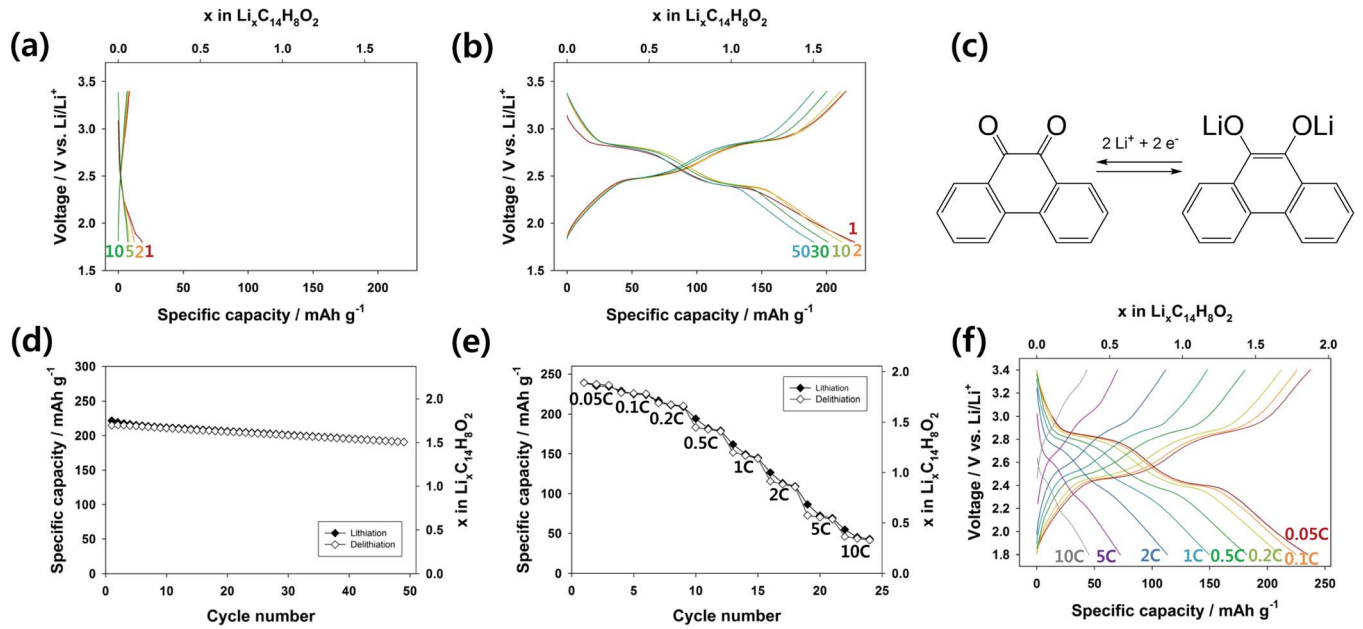

Figure 5 | Voltage profiles of (a) bare phenanthrenequinone and (b) PQ/CMK-3 for Li-ion batteries. (c) Electrochemical reaction mechanism of phenanthrenequinone. (d) Cycle performance, (e) rate capability, and (f) corresponding voltage profiles of PQ/CMK-3.

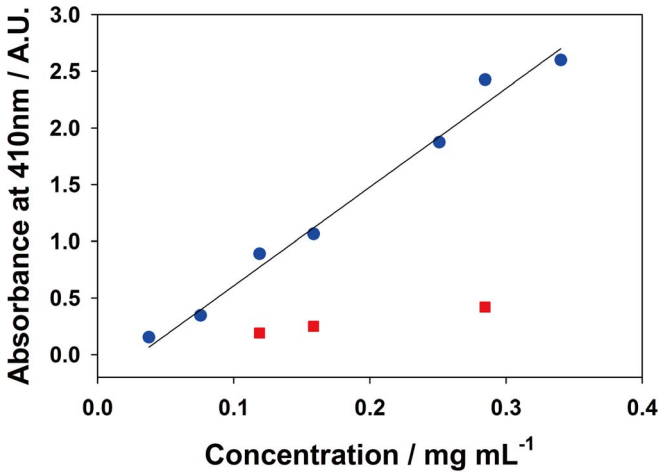

Figure 6 | Difference in absorbance between bare PQ (blue circles) and PQ/CMK-3 (red squares) at a wavelength of 410 nm after dissolution of the same amounts of PQ in TEGDME.

than CMK-3 was infiltrated. Moreover, FT-IR spectra clearly indicate the existence of the PQ in the PQ/CMK-3 (Fig. 4a). The FT-IR spectrum of PQ/CMK-3 (iii) was compared with those of neat PQ and CMK-3 (i, ii). The vibrational bands correlated with the characteristic absorptions of PQ ($\tilde{\nu}$/cm^{-1}; 1674 (C=**O**, stretch), 1591 (C=**C**, aromatic stretch), 1294, 1284, 924 (out-of-plane C−**H** bend), 764 (out-of-plane C−**H** bend), 715 (out-of-plane C−**H** bend) were observed in the PQ/CMK-3[36]. In particular, the two C-**H** bending vibrations of PQ/CMK-3 in the low energy region (715 and 764 cm^{-1}) were red-shifted and blue-shifted, respectively, compared with the neat PQ (Fig. 4b), indicating the existence of the PQ within the PQ/CMK-3 by virtue of non-covalent force (π-π stacking interaction between PQ and CMK-3). The π-π interaction is also supported by thermogravimetric analysis (TGA). As shown in Fig. 4c, all of the bare PQ evaporated before the temperature reached 270°C; in contrast, the PQ in the PQ/CMK-3 began to evaporate after the temperature reached 270°C. The difference in evaporation behavior between the bare PQ and PQ/CMK-3 is attributed to the strong π-π interaction between PQ and CMK-3 in PQ/CMK-3. The different vapour pressure between bare PQ and PQ/CMK-3 is further supported by isothermal analysis (Fig. 4d). All of the bare PQ evaporated at 250°C in 50 min, whereas the PQ in the PQ/CMK-3 did not evaporate at 250°C even after 200 min. In addition, the TGA profile of the PQ/CMK-3 indicates the loading amount of PQ in the composite range up to 31.5 wt%. Moreover, an inspection of the ^{1}H NMR spectrum of a portion of the PQ/CMK-3 after fractionating by Soxhlet extraction with chloroform revealed four resonance signals assigned to the chemical structure for the PQ (see Fig. S1 in the SI), implying that the PQ is completely stable during the infiltration process of the PQ into the CMK-3 at 250°C.

The electrochemical performance was compared with the bare PQ and PQ/CMK-3. Fig. 5a and 5b show the voltage profiles of the bare PQ and PQ/CMK-3 electrodes between 1.8 and 3.4 V at a rate of 25.7 mA g^{-1} (0.1 C rate), respectively. The PQ/CMK-3 electrode delivered a high reversible capacity of approximately 220 mA h g^{-1} at a rate of 0.1 C. However, the bare PQ electrode delivered approximately 18 mA h g^{-1}, although it was previously reported that bare PQ delivered large reversible capacity[37]. This seems to be caused by their different particle size and electrolyte species. (Note: more carbon additive (super P) was added for the preparation of the bare PQ electrodes compared to the PQ/CMK-3, and the total amount of carbon in both electrodes were same). Thus, the improved reversible capacity of the PQ/CMK-3 is attributed to the improved electrical conductivity of PQ/CMK-3. The voltage profiles exhibited reversible two-stepwise plateaus located at ca. 2.8 and 2.4 V vs. Li/Li$^+$, indicating that the insertion and deinsertion of Li$^+$ ions proceed in consecutive two-phase reactions. This implies that the PQ has two storage sites for Li$^+$ ions, which is consistent with the fact that PQ has two C=O groups. Therefore, we propose that two Li$^+$ ions are inserted into two C=O to form two C-O-Li during lithiation and vice versa (Fig. 5c). The PQ/CMK-3 also showed stable cycle performance with 89% of capacity retention over 50 cycles (Fig. 5d), which is attributed that the mesoporous carbon clearly performs well as a PQ container. The confinement of the PQ in the CMK-3 mitigated the dissolution of phenanthrenequinone in the electrolyte. This is supported by UV-VIS analysis. The same amounts of bare PQ and PQ in PQ/CMK-3 were stored in tetra(ethylene glycol) dimethyl ether (TEGDME) with stirring simultaneously. Glyme solvents are known for their good ability to dissolve organic small molecules. However, the dissolution of the PQ in PQ/CMK-3 was highly mitigated compared with that of the bare PQ, as shown in the difference in absorbance between bare PQ- and PQ/CMK-3-dissolved solvents (Fig. 6). UV-VIS spectrum of bare phenanthrenequinone is represented in Fig. S2. In addition, the rate performance of the PQ/CMK-3 was examined. It delivered approximately 113 mA h g^{-1} even at a

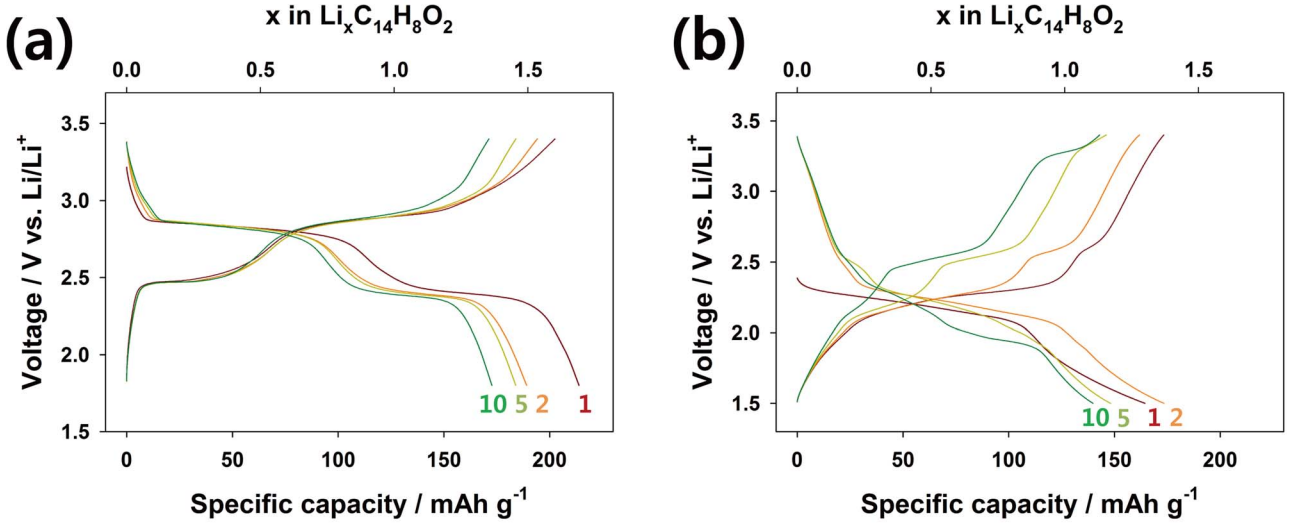

Figure 7 | Voltage profiles of (a) Phenanthrenequinone-confined Activated Carbon (PQ/AC) and (b) Anthraquinone-confined Ketjen Black (AQ/KB) for Li-ion batteries.

rate of 2 C, indicating that 51% of the reversible capacity delivered at a rate of 0.1 C is sustained (Fig. 5e). The corresponding voltage profiles of the rate performance are displayed in Fig. 5f. Furthermore, the electrochemical performance of the PQ/CMK-3 was evaluated for Na-ion batteries. The PQ/CMK-3 electrode delivered a reversible capacity of approximately 190 mA h g^{-1} at a rate of 0.1 C. However, it exhibited the poor capacity retention, which might be caused by the PQ dissolution in carbonate-based solvents or oxidative electrolyte decomposition at ca. 2.4 V vs. Na/Na^+ (Fig. S3).

The melt-diffusion-vaporization strategy base on the π-π interaction between aromatic phenanthrenequinone and carbon is generally applicable to other carbon species and small molecules such as activated carbon, ketjen black and anthraquinone. When activated carbon (AC) having a higher surface area than CMK-3 was used for the preparation of PQ-confined AC (PQ/AC), the amount of PQ in the PQ/AC composite increased to 35.9 wt.%, as shown in the TGA profiles of Fig. S4. The PQ/AC exhibited similar electrochemical performance to the PQ/CMK-3 (Fig. 7a). Anthraquinone-confined ketjen black (AQ/KB) was also successfully obtained via the melt-diffusion-vaporization strategy, and moreover, AQ/KB showed good electrochemical performance delivering the reversible capacity of about 170 mA h g^{-1} (Fig. 7b).

Discussion

We, for the first time, demonstrated that the π-π interaction-dependent vapour pressure of phenanthrenequinone can be used to synthesize a nanostructured mesoporous carbon-phenanthrenequinone composite with enhanced electrochemical performance due to the confinement effects. Intimate contact between the insulating phenanthrenequinone and the conductive carbon framework at nanoscale dimensions improves the electrical conductivity. This enables a more complete redox reaction to take place, achieving enhanced utilization of the electrochemically active phenanthrenequinone. This results in the improved reversible capacity of 240 mA h g^{-1} at a rate of 0.05 C, almost reaching the theoretical specific capacity (257 mA h g^{-1}). The confinement of the phenanthrenequinone in the mesoporous carbon further mitigated the diffusion of the dissolved phenanthrenequinone out of the mesoporous carbon framework, minimized the loss of the electrochemically active mass and improved the cycling performance with little capacity fading over 50 cycles.

Methods

Synthesis. CMK-3 was synthesized according to the reported procedure[38]. The PQ/CMK-3 nanocomposite was prepared by following a melt-diffusion-vaporization strategy. CMK-3 (0.5 g) and 9,10-phenanthrenequinone (1.5 g, Sigma Aldrich) were ground together, pelletized, and heated at 250°C for 3 h in air. The PQ/AC composite was also synthesized at the same condition. For the preparation of the AQ/KB composite, the mixture of AQ and KB was heated at 300°C.

Material characterization. SEM samples were examined using a Hitachi S-4800 field-emission scanning electron microscope (FE-SEM). High-resolution TEM samples were investigated using a high resolution transmission electron microscope (HR-TEM, STEM, JEOL ARM-200F) having a probe Cs aberration corrector (CEOS GmbH) and an energy-dispersive X-ray spectroscopy (EDS, Oxford Instruments X-MaxN 80 TLE) attached to the TEM. The porous structures of the samples were analyzed in a nitrogen adsorption experiment at −196°C using a BEL BELSORP-Max system. The surface areas and pore sizes of the samples were calculated using the Brunauer-Emmett-Teller (BET) equation and the Barrett-Joyner-Halenda (BJH) method, respectively. Infrared spectra were recorded by a Varian 670-IR spectrometer equipped with an attenuated total reflectance (ATR) device. Nuclear magnetic resonance (NMR) spectra were recorded by an Agilent 400 MHz spectrophotometer using $CDCl_3$ as the solvent and tetramethylsilane (TMS) as the internal standard. A thermal analysis was performed at a heating rate of 5°C min^{-1} in a nitrogen atmosphere using a thermogravimetric analyzer (TGA, SDT Q600). Isothermal analysis was performed at 250°C. The dissolution of PQ and PQ/CMK-3 in TEGDME was investigated by ultraviolet-visible (UV-VIS) spectroscopy (Varian, Cary 5000).

Electrochemical characterization. Samples of the PQ/CMK-3 and bare PQ were mixed with carbon black (Super P) and carboxymethyl cellulose (CMC) in 8 : 0.5 : 1.5 and 3 : 5 : 2 weight ratios, respectively, in order to use the same ratio of PQ: carbon: binder for the fabrication of electrodes. Samples of the PQ/AC and AQ/KB were mixed with carbon black (Super P) and carboxymethyl cellulose (CMC) in an 8 : 0.5 : 1.5 weight ratio for the fabrication of electrodes. The slurry was casted onto a current collector (Al). The electrodes were dried at 120°C in a vacuum oven overnight. Their electrochemical characteristics for Li-ion batteries were evaluated using 2016 coin cells with a Li metal anode and 1.3 M LiTFSI in a tetraethylene glycol dimethyl ether (TEGDME) electrolyte solution. A microporous polyolefin film was used as a separator. Galvanostatic experiments were performed at a current density of 25.7 mA g^{-1} (ca. 0.1 C) and 30°C. In addition, their electrochemical characteristics for Na-ion batteries were evaluated using 2032 coin cells with a Na metal anode and 1 M $NaPF_6$ in a mixed solvent of ethylene carbonate and propylene carbonate (1/1 v/v).

1. Armand, M. & Tarascon, J. M. Building better batteries. *Nature* **451**, 652–657 (2008).
2. Tarascon, J. M. & Armand, M. Issues and challenges facing rechargeable lithium batteries. *Nature* **414**, 359–367 (2001).
3. Ellis, B. L., Lee, K. T. & Nazar, L. F. Positive Electrode Materials for Li-Ion and Li-Batteries. *Chem. Mater.* **22**, 691–714 (2010).
4. Liang, Y., Zhang, P. & Chen, J. Function-oriented design of conjugated carbonyl compound electrodes for high energy lithium batteries. *Chem. Sci.* **4**, 1330–1337 (2013).
5. Liang, Y., Tao, Z. & Chen, J. Organic Electrode Materials for Rechargeable Lithium Batteries. *Adv. Energy Mater.* **2**, 742–769 (2012).
6. Tarascon, J. M. Key challenges in future Li-battery research. *Phil. Trans. R. Soc. A* **368**, 3227–3241 (2010).
7. Han, X., Qing, G., Sun, J. & Sun, T. How many lithium ions can be inserted onto fused C6 aromatic ring systems? *Angew. Chem. Int. Ed.* **51**, 5147–5151 (2012).
8. Hanyu, Y. & Honma, I. Rechargeable quasi-solid state lithium battery with organic crystalline cathode. *Sci. Rep.* **2**, 453 (2012).
9. Chen, H. *et al.* From biomass to a renewable Li(x)C(6)O(6) organic electrode for sustainable Li-ion batteries. *ChemSusChem* **1**, 348–355 (2008).
10. Williams, D. L., Byrne, J. J. & Driscoll, J. S. A High Energy Density Lithium/Dichloroisocyanuric Acid Battery System. *J. Electrochem. Soc.* **116**, 2–4 (1969).
11. Walker, W. *et al.* The effect of length and cis/trans relationship of conjugated pathway on secondary battery performance in organolithium electrodes. *Electrochem. Commun.* **12**, 1348–1351 (2010).
12. Armand, M. *et al.* Conjugated dicarboxylate anodes for Li-ion batteries. *Nat. Mater.* **8**, 120–125 (2009).
13. Chen, H. *et al.* Lithium Salt of Tetrahydroxybenzoquinone: Toward the Development of a Sustainable Li-Ion Battery. *J. Am. Chem. Soc.* **131**, 8984–8988 (2009).
14. Chen, H. *et al.* From Biomass to a Renewable LiXC6O6 Organic Electrode for Sustainable Li-Ion Batteries. *ChemSusChem* **1**, 348–355 (2008).
15. Renault, S., Geng, J., Dolhem, F. & Poizot, P. Evaluation of polyketones with N-cyclic structure as electrode material for electrochemical energy storage: case of pyromellitic diimide dilithium salt. *Chem. Commun.* **47**, 2414–2416 (2011).
16. Han, X., Chang, C., Yuan, L., Sun, T. & Sun, J. Aromatic Carbonyl Derivative Polymers as High-Performance Li-Ion Storage Materials. *Adv. Mater.* **19**, 1616–1621 (2007).
17. Geng, J. Q., Bonnet, J.-P., Renault, S., Dolhem, F. & Poizot, P. Evaluation of polyketones with N-cyclic structure as electrode material for electrochemical energy storage: case of tetraketopiperazine unit. *Energy Environ. Sci.* **3**, 1929–1933 (2010).
18. Liang, Y., Zhang, P., Yang, S., Tao, Z. & Chen, J. Fused Heteroaromatic Organic Compounds for High-Power Electrodes of Rechargeable Lithium Batteries. *Adv. Energy Mater.* **3**, 600–605 (2013).
19. Reddy, A. L. *et al.* Lithium storage mechanisms in purpurin based organic lithium ion battery electrodes. *Sci. Rep.* **2**, 960 (2012).
20. Sharma, P., Damien, D., Nagarajan, K., Shaijumon, M. M. & Hariharan, M. Perylene-polyimide-Based Organic Electrode Materials for Rechargeable Lithium Batteries. *J. Phys. Chem. Lett.* **4**, 3192–3197 (2013).
21. Yao, M., Yamazaki, S., Senoh, H., Sakai, T. & Kiyobayashi, T. Crystalline polycyclic quinone derivatives as organic positive-electrode materials for use in rechargeable lithium batteries. *Mater. Sci. Eng., B* **177**, 483–487 (2012).
22. Wu, H., Wang, K., Meng, Y., Lu, K. & Wei, Z. An organic cathode material based on a polyimide/CNT nanocomposite for lithium ion batteries. *J. Mater. Chem. A* **1**, 6366–6372 (2013).
23. Le Gall, T., Reiman, K. H., Grossel, M. C. & Owen, J. R. Poly(2,5-dihydroxy-1,4-benzoquinone-3,6-methylene): a new organic polymer as positive electrode material for rechargeable lithium batteries. *J. Power Sources* **119**, 316–320 (2003).
24. Liu, K., Zheng, J., Zhong, G. & Yang, Y. Poly(2,5-dihydroxy-1,4-benzoquinonyl sulfide) (PDBS) as a cathode material for lithium ion batteries. *J. Mater. Chem.* **21**, 4125–4131 (2011).
25. Song, Z., Zhan, H. & Zhou, Y. Polyimides: promising energy-storage materials. *Angew. Chem. Int. Ed.* **49**, 8444–8448 (2010).

26. Lin, H.-C., Li, C.-C. & Lee, J.-T. Nitroxide polymer brushes grafted onto silica nanoparticles as cathodes for organic radical batteries. *J. Power Sources* **196**, 8098–8103 (2011).
27. Nokami, T. *et al.* Polymer-bound pyrene-4,5,9,10-tetraone for fast-charge and -discharge lithium-ion batteries with high capacity. *J. Am. Chem. Soc.* **134**, 19694–19700 (2012).
28. Oyaizu, K., Choi, W. & Nishide, H. Functionalization of poly(4-chloromethylstyrene) with anthraquinone pendants for organic anode-active materials. *Polym. Adv. Technol.* **22**, 1242–1247 (2011).
29. Chen, H. *et al.* Electrochemical Reactivity of Lithium Chloranilate vs Li and Crystal Structures of the Hydrated Phases. *Electrochem. Solid-State Lett.* **12**, A102–A106 (2009).
30. Park, Y. *et al.* Sodium Terephthalate as an Organic Anode Material for Sodium Ion Batteries. *Adv. Mater.* **24**, 3562–3567 (2012).
31. Lei, Z. *et al.* A MC/AQ Parasitic Composite as Cathode Material for Lithium Battery. *J. Electrochem. Soc.* **158**, A991–A996 (2011).
32. Li, B. *et al.* Manipulating the Electronic Structure of Li-Rich Manganese-Based Oxide Using Polyanions: Towards Better Electrochemical Performance. *Adv. Funct. Mater.* **24**, 5112–5118 (2014).
33. Luo, C. *et al.* Graphene oxide wrapped croconic acid disodium salt for sodium ion battery electrodes. *J. Power Sources* **250**, 372–378 (2014).
34. Lee, M. *et al.* Organic Nanohybrids for Fast and Sustainable Energy Storage. *Adv. Mater.* **26**, 2558–2565 (2014).
35. Ji, X., Lee, K. T. & Nazar, L. F. A highly ordered nanostructured carbon-sulphur cathode for lithium-sulphur batteries. *Nat. Mater.* **8**, 500–506 (2009).
36. Muddasir, H. *et al.* Molecular Properties of 9,10-Phenanthrenequinone and Benzil. *Chem. Res. Chin. Univ.* **25**, 950–956 (2009).
37. Tobishima, S. i., Yamaki, J. i. & Yamaji, A. Cathode Characteristics of Organic Electron Acceptors for Lithium Batteries. *J. Electrochem. Soc.* **131**, 57–63 (1984).
38. Jun, S. *et al.* Synthesis of New, Nanoporous Carbon with Hexagonally Ordered Mesostructure. *J. Am. Chem. Soc.* **122**, 10712–10713 (2000).

Acknowledgments

This research was supported by the National Research Foundation of Korea (NRF) grant funded by the Korea Government (MSIP and MOE) (No. 2010-0019408 and No. NRF-2013R1A1A2013446), by the MSIP (Ministry of Science, ICT&Future Planning), Korea, under the C-ITRC(Convergence Information Technology Research Center) support program (NIPA-2013-H0301-13-1009) supervised by the NIPA(National IT Industry Promotion Agency), and by Korea Electrotechnology Research Institute (KERI) Primary research program through the National Research Council of Science & Technology funded by the Ministry of Science, ICT and Future Planning (MSIP) (No. 14-12-N0101-69).

Author contributions

M.S.K., C.Y. and K.T.L. designed the research, performed the experiments, and wrote the paper. A.C. and Y.P. advised the experimental design of the synthesis of a phenanthrenequinone-confined CMK-3 and experimental measurements, and the interpretation of results. J.Y.C. synthesized ordered mesoporous carbon (CMK-3). S.H.J. commented on the manuscript. Y.N.J. and Y.J.K. performed TEM analysis. H.K. and S.Y.H. performed NMR analysis. K.T.L. supervised the overall experimental design and writing.

Additional information

Supplementary information accompanies this paper at http://www.nature.com/scientificreports

Competing financial interests: The authors declare no competing financial interests.

How to cite this article: Kwon, M.-S. *et al.* Synthesis of Ordered Mesoporous Phenanthrenequinone-Carbon via π-π Interaction-Dependent Vapor Pressure for Rechargeable Batteries. *Sci. Rep.* **4**, 7404; DOI:10.1038/srep07404 (2014).